



■ **BIOMECHANICS**

The effect of malalignment on proximal tibial strain in fixed-bearing unicompartmental knee arthroplasty

A COMPARISON BETWEEN METAL-BACKED AND ALL-POLYETHYLENE COMPONENTS USING A VALIDATED FINITE ELEMENT MODEL

**I. Danese,
P. Pankaj,
C. E. H. Scott**

University of
Edinburgh, Edinburgh,
United Kingdom

Objectives

Elevated proximal tibial bone strain may cause unexplained pain, an important cause of uni-compartmental knee arthroplasty (UKA) revision. This study investigates the effect of tibial component alignment in metal-backed (MB) and all-polyethylene (AP) fixed-bearing medial UKAs on bone strain, using an experimentally validated finite element model (FEM).

Methods

A previously experimentally validated FEM of a composite tibia implanted with a cemented fixed-bearing UKA (MB and AP) was used. Standard alignment (medial proximal tibial angle 90°, 6° posterior slope), coronal malalignment (3°, 5°, 10° varus; 3°, 5° valgus), and sagittal malalignment (0°, 3°, 6°, 9°, 12°) were analyzed. The primary outcome measure was the volume of compressively overstressed cancellous bone (VOCB) <math><-3000 \mu\epsilon</math>. The secondary outcome measure was maximum von Mises stress in cortical bone (MSCB) over a medial region of interest.

Results

Varus malalignment decreased VOCB but increased MSCB in both implants, more so in the AP implant. Varus malalignment of 10° reduced the VOCB by 10% and 3% in AP and MB implants but increased the MSCB by 14% and 13%, respectively. Valgus malalignment of 5° increased the VOCB by 8% and 4% in AP and MB implants, with reductions in MSCB of 7% and 10%, respectively. Sagittal malalignment displayed negligible effects. Well-aligned AP implants displayed greater VOCB than malaligned MB implants.

Conclusion

All-polyethylene implants are more sensitive to coronal plane malalignments than MB implants are; varus malalignment reduced cancellous bone strain but increased anteromedial cortical bone stress. Sagittal plane malalignment has a negligible effect on bone strain.

Cite this article: *Bone Joint Res* 2019;8:55–64.

Keywords: Unicompartmental knee arthroplasty, Malalignment, Bone strain, Finite element analysis

■ I. Danese, MEng, Engineering Masters Student,

■ P. Pankaj, PhD, Professor of Numerical Modelling, School of Engineering, University of Edinburgh, Edinburgh, UK.

■ C. E. H. Scott, MSc, FRCS(Tr&Orth), MD, Consultant Orthopaedic Surgeon, NRS Clinical Research Fellow, School of Engineering, University of Edinburgh, Edinburgh, UK; Department of Orthopaedics, Royal Infirmary of Edinburgh, Edinburgh, UK.

Correspondence should be sent to C. E. H. Scott; email: chloe.scott@nhslothian.scot.nhs.uk

doi: 10.1302/2046-3758.82.BJR-2018-0186.R2

Bone Joint Res 2019;8:55–64.

Article focus

■ Finite element investigation of the effect of unicompartmental knee arthroplasty (UKA) tibial component alignment on cancellous and cortical bone strains and stresses in both metal-backed (MB) and all-polyethylene (AP) implants.

Key messages

■ Coronal plane malalignment affects bone strain more than sagittal malalignment, and this is more marked in AP UKA implants than in MB implants.

■ Well-aligned AP implants display greater bone strains than malaligned MB implants.

Strengths and limitations

■ The strength of this finite element study is that it permits examination of bone strain for a wide range of malalignment scenarios for two different UKA implants.
 ■ Limitations of this study include the use of composite tibias, the performance of a linearly elastic analysis, and the lack of kinematic analysis.

Introduction

The survival of unicompartmental knee arthroplasty (UKA) remains variable between implants and institutions, with joint registries reporting ten-year survival ranging from 80% to 96%.¹⁻³ The strong relationship between surgeon volume and UKA survivorship^{4,5} implies that achieving well-aligned congruent UKAs is key to maximizing survival. Unexplained pain is a significant cause of UKA revision, with between 24% and 48% of revisions performed for this indication.^{6,7} Elevated proximal tibial strain and microdamage may contribute to this pain.^{8,9} Joint registries do not distinguish between metal-backed (MB) and all-polyethylene (AP) UKAs, but both experimental data^{10,11} and finite element analysis (FEA)¹² have shown elevated proximal tibial bone strain in AP UKAs compared with MB medial UKAs.

Finite element analysis has been used previously to investigate the influence of component alignment on cortical bone strain in MB implants.¹³⁻¹⁵ Both coronal plane varus malalignment^{13,14} and valgus malalignment¹⁵ have been associated with elevated cortical bone strains in FEAs of a MB mobile-bearing UKA implant. In a MB fixed-bearing implant, mild valgus malalignment of between 2° and 4° has been associated with a reduction in cancellous bone strain.¹³ Cortical rim support has also been identified as an important predictor of bone strain, with both overhang and underhang associated with elevated cortical bone strains again in a MB mobile-bearing UKA implant.¹⁴ We have previously shown elevated cancellous bone strains in AP UKAs, compared with MB UKAs, in optimal alignment,^{11,12} in addition to an increased revision rate for unexplained pain.¹⁶ To our knowledge, no investigation of the influence of metal backing and malalignment has been published.

The aims of this study were to investigate the effect of medial UKA tibial component alignment on bone strain in both MB and AP implants. We hypothesized that bone strains beneath AP components would be more reactive to malalignment than the bone beneath MB implants.

Materials and Methods

A finite element model (FEM) previously experimentally validated using digital image correlation ($\pm 4.5\%$ error) and acoustic emissions ($\pm 12.5\%$ error) was used.¹² This consisted of a third-generation left composite tibia with cortical and cancellous parts and fixed-bearing UKAs of 8 mm thickness (SIGMA Partial; DePuy Synthes, Raynham, Massachusetts) with 1.5 mm cement mantles (Fig. 1). Different component alignments were analyzed using Abaqus CAE Version 6.12 (Simulia, Dassault Systèmes Simulia Corp., Waltham, Massachusetts).

Anatomical axes were defined in coronal and sagittal planes.¹⁷ The tibia was cut distally 200 mm below the intercondylar eminence to reduce computational effort. Proximal medial bony resections of 6 mm were made in

various alignments. The neutral alignment was 90° in the coronal plane with 6° of posterior slope in the sagittal plane. The following malalignments were investigated: 3°, 5°, and 10° varus; 3° and 5° valgus; and 0°, 3°, 9°, and 12° of posterior slope.

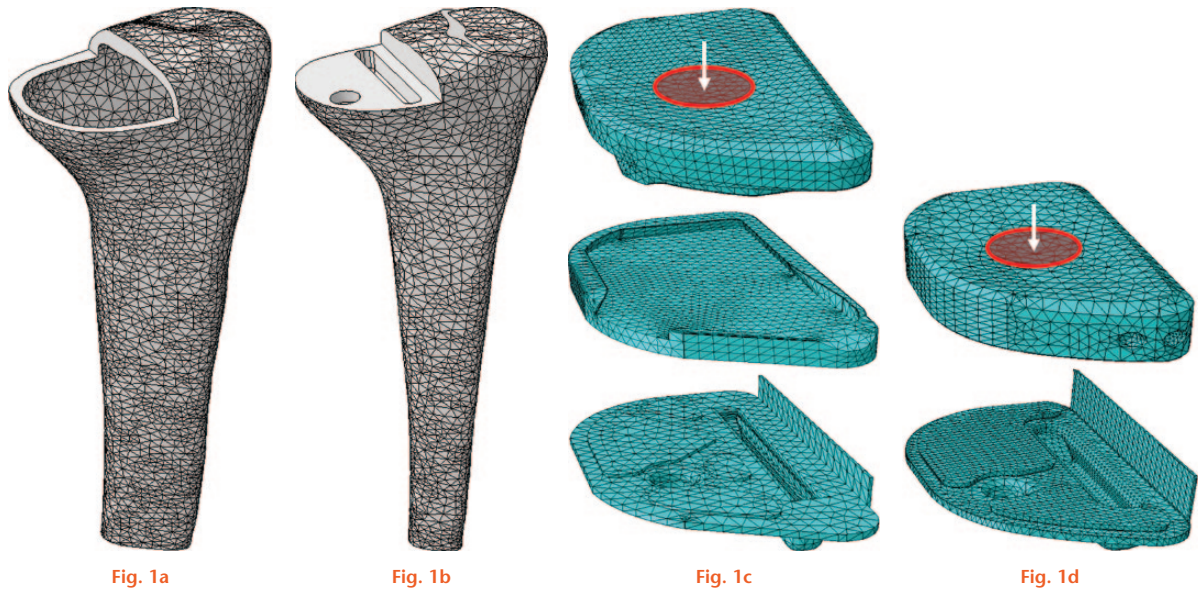
All materials used in the FE model were assumed to exhibit isotropic, homogeneous, and linearly elastic material behaviour. Material properties are shown in Table I. Linear tetrahedral meshes with mean internodal distances of 1.5 mm to 2.0 mm were used. Mesh resolution was based on a 2% convergence criterion for the displacement magnitudes in the proximal tibia (Table I, Fig. 1). Mesh convergence studies showed a convergence of <1.2% between element sizes of 1.5 mm and 2.5 mm; 2 mm was therefore chosen for cortical and cancellous bone (Table I). Tie constraints were used to bond cement to bone and tibial insert to metal baseplate.¹⁸ The distal tibia was fully restrained. Proximally, the tibia was restrained against medial/lateral and anterior/posterior translations at a node representing the anterior cruciate ligament (ACL) footprint to prevent non-physiological bending.

Load was applied directly to the polyethylene articular surface medially and to the lateral tibial plateau, in order to replicate previous biomechanical testing, as distributed loads over a circle with a radius of 6 mm centred at the centre point of each polyethylene/plateau.¹¹ A 60:40 medial:lateral load division¹⁹ was used, and a 2500 N medial load (4170 N maximum total load) was applied over five equal 500 N increments. This maximum load was approximately six times body weight (70 kg) and reflects physiological tibiofemoral loading.²⁰ Results are presented for 1000 N and 2500 N medial loads (1668 N and 4170 N total loads).

The primary outcome measure was the volume of compressively overstressed cancellous bone (VOCB) experiencing minimum principal strain of less than $-3000\mu\epsilon$, representing pathological overloading.²¹ This limit has been used as a strain criterion previously.¹² In accordance with the commonly used convention in engineering, the negative sign denotes compression and positive tension. Secondary outcomes included maximum von Mises stress in cortical bone (MSCB). This was measured over a region of interest overlying the anteromedial tibia, as previously used by Simpson et al,⁸ at the location frequently associated with patient reports of pain (Fig. 2).

Results

Standard alignment. The AP tibial component generated a greater VOCB than the MB tibial component (Table II), with VOCB distributed over a larger part of the resected cancellous bone surface and extending deeper into it. For the MB implant, the VOCB was generated primarily at the implant peg and keel. Numerical data are displayed in Table II. Even when correctly aligned, there was



The finite element model: a) cortical bone part; b) cancellous bone part; c) metal-backed implant (polyethylene, metal tray) and cement meshes; and d) all-polyethylene implant and cement mesh. The area of distributed load is highlighted.

Table I. Material properties and elements for parts in the standard alignment models. Cortical and cancellous bone properties apply to loading in compression

Part	Elastic modulus, GPa	Poisson's ratio	Internodal distance, mm	Elements, n
All-polyethylene (AP)				
Cortical bone	16.7	0.3	2	108 542
Cancellous bone	0.155	0.3	2	96 573
PMMA cement	2.4	0.3	1.5	19 691
AP tibia	0.69	0.46	2	21 496
Metal-backed (MB)				
Cortical bone	16.7	0.3	2	105 984
Cancellous bone	0.155	0.3	2	99 485
PMMA cement	2.4	0.3	1.5	25 630
MB tibial tray (CoCr)	210	0.3	1.5	19 851
Polyethylene insert	0.69	0.46	1.5	25 630

PMMA, poly(methyl methacrylate); CoCr, cobalt chromium

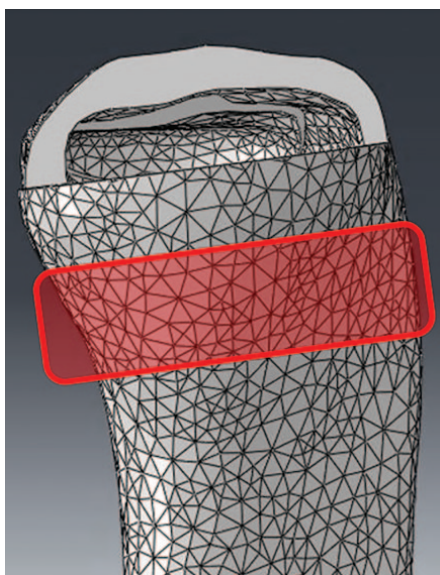


Fig. 2

Region of interest for maximum von Mises stress in cortical bone.

a substantial difference in VOCB between the two tibial components at all loads (Table II).

Coronal malalignment. Figures 3a and 3b show the VOCB and the MSCB in the anteromedial tibia for both implants at medial loads of 2500N and 1000N, respectively. The VOCB under the MB tibial component was lower than for the AP in all scenarios. In fact, even a poorly aligned MB tibial component yielded a smaller VOCB compared with a perfectly aligned AP component (Fig. 4). Overall, the MB implant was less sensitive to coronal plane malalignment in terms of VOCB than the AP implant, with 2% to 6% increases in VOCB compared with 5% to 10% increases in the AP tibial component (Table III).

The absolute VOCB was much lower for the 1000N medial load case compared with the 2500N medial load case (Fig. 3); for the lower load, the two tibial components only yielded 34% (AP) and 20% (MB) of the VOCB found for the higher load.

Standard alignment was not associated with the lowest cancellous bone strains (VOCB) in either implant.

Table II. The volume of compressively overstrained cancellous bone (VOCB, minimum principal strain) in all-polyethylene (AP) and metal-backed (MB) tibial components in standard alignment

Medial load, N	Total load, N	Strain value, $\mu\epsilon$	AP VOCB, mm^3	MB VOCB, mm^3	% increase in VOCB for AP
1000	1668	< -3000	9744	4310	+ 126.1
2500	4170	< -3000	28 449	21 876	+ 30.0

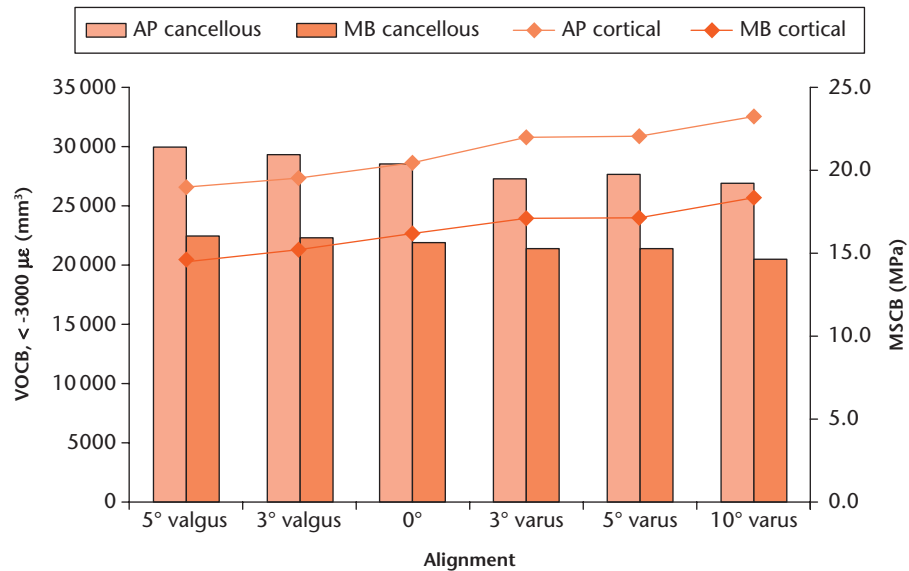


Fig. 3a

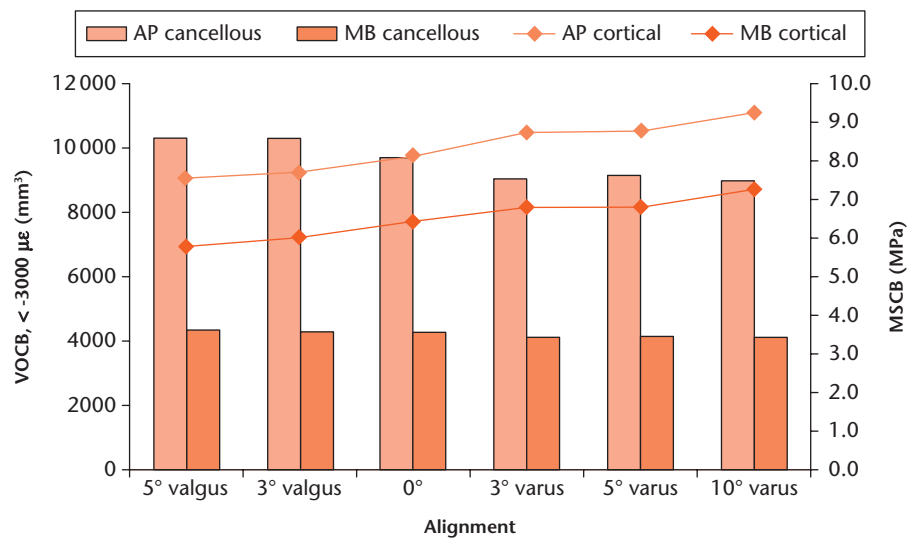


Fig. 3b

Coronal plane malalignment. The volume of compressively overstrained cancellous bone (VOCB, <math>< -3000 \mu\epsilon</math>) and the anteromedial maximum von Mises stress in cortical bone (MSCB) for all-polyethylene (AP) and metal-backed (MB) implants at medial loads of a) 2500 N and b) 1000 N. Bars (left-hand y-axis) represent the VOCB and lines (right-hand y-axis) represent the MSCB.

Increasing varus alignment reduced VOCB, but this was balanced by a reciprocal increase in MSCB. This is highlighted in Figure 3 and by the contour maps in Figure 4. The same pattern existed for both compressive (minimum principal) and tensile (maximum principal) strains (Fig. 5). The MB tibial component distributes load more

uniformly over the resected surface. Stress and strain concentrations are therefore less pronounced for the MB implant than for the AP implant. This explains why a higher MSCB was seen for the AP tibial component, even though the load-bearing support of the cortical bone was less for the AP implant than for the MB implant. Standard

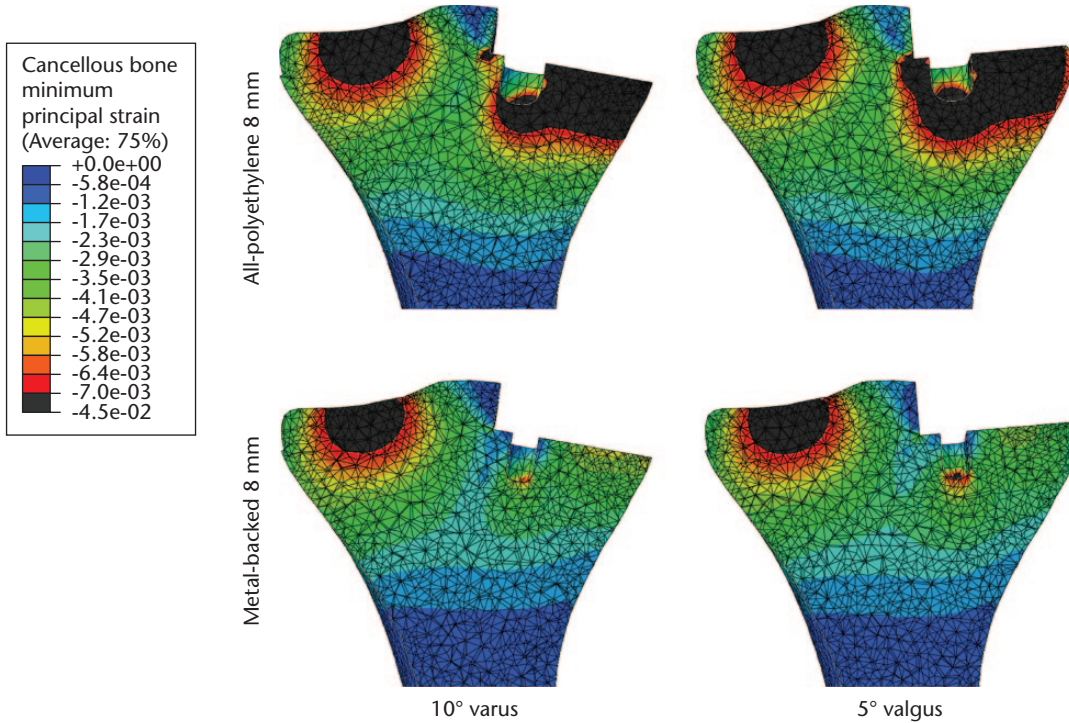


Fig. 4

Mid-coronal plane contour maps showing for all-polyethylene and metal-backed implants in varus and valgus malalignment at a medial load of 2500 N.

Table III. The volume of compressively overstrained cancellous bone (VOCB, <-3000 µε) by implant and alignment for a medial load of 2500 N

Alignment	All-polyethylene implant				Metal-backed implant			
	VOCB, mm ³	% diff.	MSCB, MPa	% diff.	VOCB, mm ³	% diff.	MSCB, MPa	% diff.
Coronal plane								
5° valgus	29 860	+5.0	18.9	-7.1	22 502	+2.9	14.6	-9.7
3° valgus	29 300	+3.0	19.5	-4.4	22 325	+2.1	15.2	-6.1
0**	28 449	0.0	20.4	0.0	21 876	0.0	16.2	0.0
3° varus	27 275	-4.1	21.9	+7.7	21 324	-2.5	17.1	+5.9
5° varus	27 582	-3.0	22.0	+7.9	21 365	-2.3	17.1	+5.8
10° varus	26 882	-5.5	23.2	+13.9	20 516	-6.2	18.3	+13.3
Sagittal plane								
0°	29 643	+4.2	7.9	-3.4	21 833	-0.2	6.6	+2.3
3°	28 374	-0.3	8.0	-2.2	22 070	+0.9	6.5	+0.7
6**	28 449	0.0	8.2	0.0	21 876	0.0	6.5	0.0
9°	28 287	-0.6	8.3	+2.4	21 772	-0.5	6.3	-1.8
12°	28 473	+0.1	8.5	+4.3	21 707	-0.8	6.5	0.0

*Standard % difference compared with standard alignment
diff., difference; MSCB, maximum von Mises stress in cortical bone

alignment appears to represent balance between cancellous bone strain and cortical bone stress.

Sagittal malalignment. Changes in tibial slope had negligible effects on both VOCB and MSCB compared with coronal plane malalignments. A standard 6° posterior tibial slope produced the least VOCB. Both neutral slope (0°) and excessive slope (12°) increased the VOCB at medial loads of 1000 N and 2500 N by small amounts (Table III, Figs 6a and 6b). The MSCB increased as the slope increased in the AP implant but not in the MB implant. Considering that these differences are small, approaching values close to the mesh convergence criteria (<1.2%), it

can be concluded that sagittal plane malalignment is not detrimental to proximal tibial bone strain, neither for the AP nor for the MB tibial component in this model loaded without the femur.

Although the absolute cancellous strain and cortical stress differ little with sagittal alignment, contour maps show that the locations of stress/strain concentrations are affected by sagittal alignment (Fig. 7). Cancellous bone strain shifts posteriorly with increasing posterior slope, more so in the AP implant. Again, the MB tibial component yielded less VOCB, with concentrations primarily at the peg and keel. The small amount of

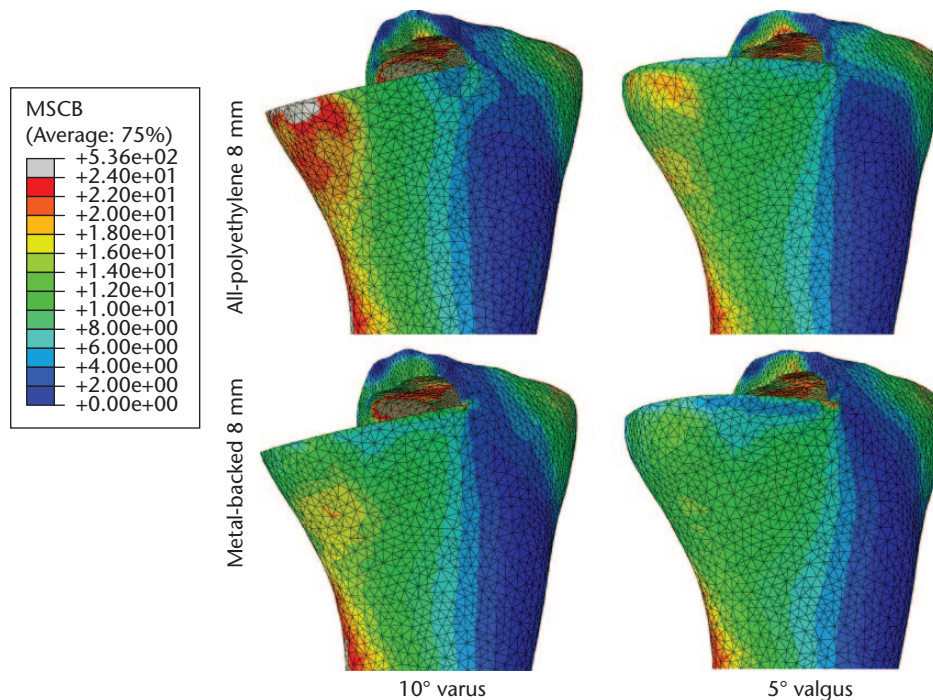


Fig. 5

Anteromedial contour maps showing von Mises stress in cortical bone (MSCB) for all-polyethylene and metal-backed implants in varus and valgus malalignment at a medial load of 2500 N.

variation in the MSCB with sagittal malalignment reflects constant cortical support across these malalignments (Figs 6a and 6b).

Discussion

Malalignment had less effect on the VOCB than implant selection; well-aligned AP implants displayed greater volumes of overstrained cancellous bone and greater anteromedial MSCB than poorly aligned MB implants at low and high loads. Coronal plane alignment had a greater influence on bone strain and stress than sagittal plane alignment, and AP implants were more sensitive to malalignment than MB implants. A balance appears to exist between cancellous bone strain and cortical bone stress; contour maps and numerical data suggest that increasing cancellous bone strain concentrations are offset by decreasing cortical bone stress concentrations, and *vice versa* for coronal plane malalignment. For both implants, valgus malalignment was associated with higher volumes of overstrained cancellous bone but lower cortical bone stresses. Varus malalignment led to lower volumes of overstrained cancellous bone, but greater maximum anteromedial cortical bone stresses. Our results suggest that although inaccurate alignment of the tibial component does affect cancellous bone strain, the effect of the selected tibial component material is much greater.

Our findings of increasing cortical stresses in varus malalignment and increasing cancellous strains in valgus malalignment are similar to the findings of Simpson

et al¹⁴ and Sawatari et al.¹³ Simpson et al¹⁴ found that increasing varus alignment led to the largest increase in mean von Mises stress in cortical bone, with a 14% increase from the standard alignment to 2° varus, while a 2° valgus malalignment yielded only a 4% increase. Sawatari et al¹³ reported a 77% increase in the yield area of the cancellous bone at the resected surface when a MB tibial component was malaligned from 0° to 6° varus, with a decrease of 30% with 4° of valgus. With increasing varus malalignment, the cancellous bone strain concentration shifts medially, resulting in more support from the cortical bone, thus lowering cancellous strains and increasing cortical stresses.

It may be expected that stiffer MB implants, which shield the cancellous bone from compressive stresses and strains, convey more to the cortical bone. In our model, cortical bone stresses were consistently higher in the AP implants. Our use of tie constraints between bone and cement may have led to an overestimation of cortical stresses, as less stiff AP implants bend more under load. While we employed minimum principal strain for cancellous bone regions considered in this study (as the strain state is expected to be largely compressive), the cortical bone can experience both tension and compression due to possible bending (previous biomechanical testing indicated tensile and compressive strains over the proximal tibial cortex).¹¹ We chose von Mises stress to examine the stress state, since it is perhaps the most demonstrative scalar measure in stress state evaluation within a

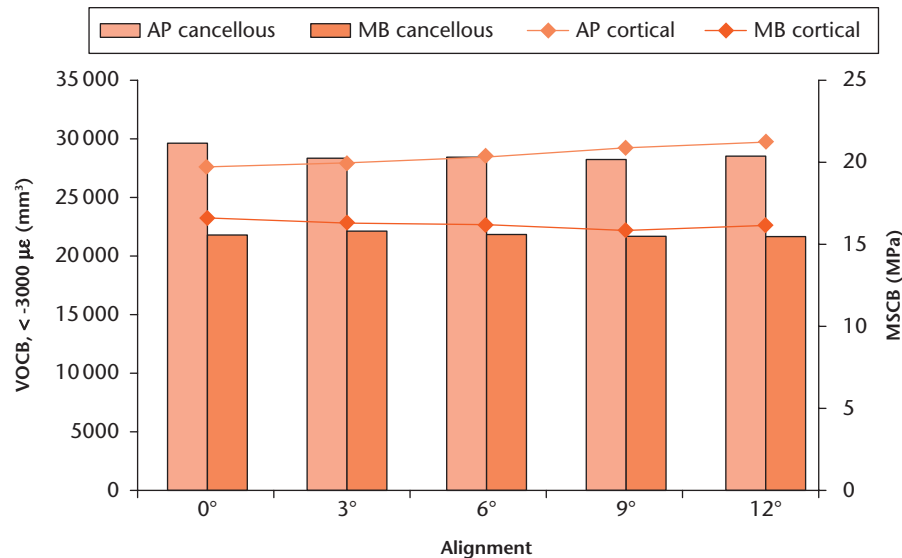


Fig. 6a

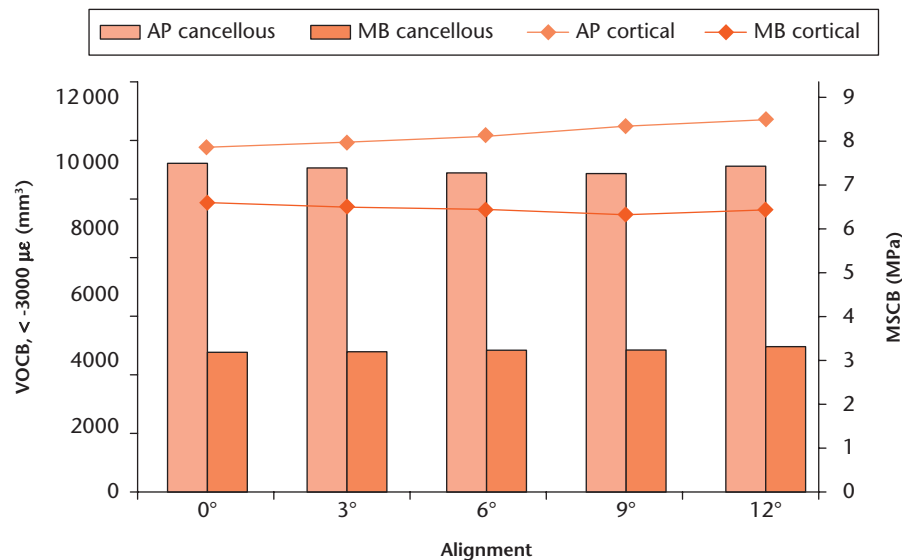


Fig. 6b

Sagittal plane malalignment: the volume of compressively overstrained cancellous bone (VOCB) (<math>< -3000 \mu\epsilon</math>) and the anteromedial maximum von Mises stress in cortical bone (MSCB) for all-polyethylene (AP) and metal-backed (MB) implants at medial loads of a) 2500 N and b) 1000 N. The VOCB is represented by bars (left-hand y-axis) and the MSCB by lines (right-hand y-axis).

material (and is an important constituent of almost all yield criteria) and accounts for both tensile and compressive stresses. Also, von Mises stress enables comparison with much of the literature.

Joint registries do not distinguish between AP and MB UKA implants. Poor survivorship of AP UKAs has been reported,²²⁻²⁵ with early failures commonly experienced due to tibial loosening, subsidence, or pain. The increased sensitivity to malalignment demonstrated here in AP implants may well contribute to these modes of failure. It is uncertain whether greater cancellous bone strain translates into poorer clinical outcome, but greater strains with ongoing microfracture and remodelling may be the cause of unexplained pain, which is a larger problem in

AP than in MB UKAs.⁹ Our previous FEA of AP and MB UKAs demonstrated a significant effect of polyethylene thickness in AP but not in MB implants.¹² Malalignment was investigated here using 8 mm components only. It could be expected that the effects of coronal plane malalignment would be magnified with thinner implants. Although excessive or neutral tibial slope had little effect on bone strains, its influence is undoubtedly exerted kinematically with flexion instability or stiffness rather than bone strain concentrations.

The advent of robotic UKA offers improved implant alignment with less variability.²⁶ This technology is based around fixed-bearing implants, and may well help to narrow the market gap between mobile-bearing (66% of the

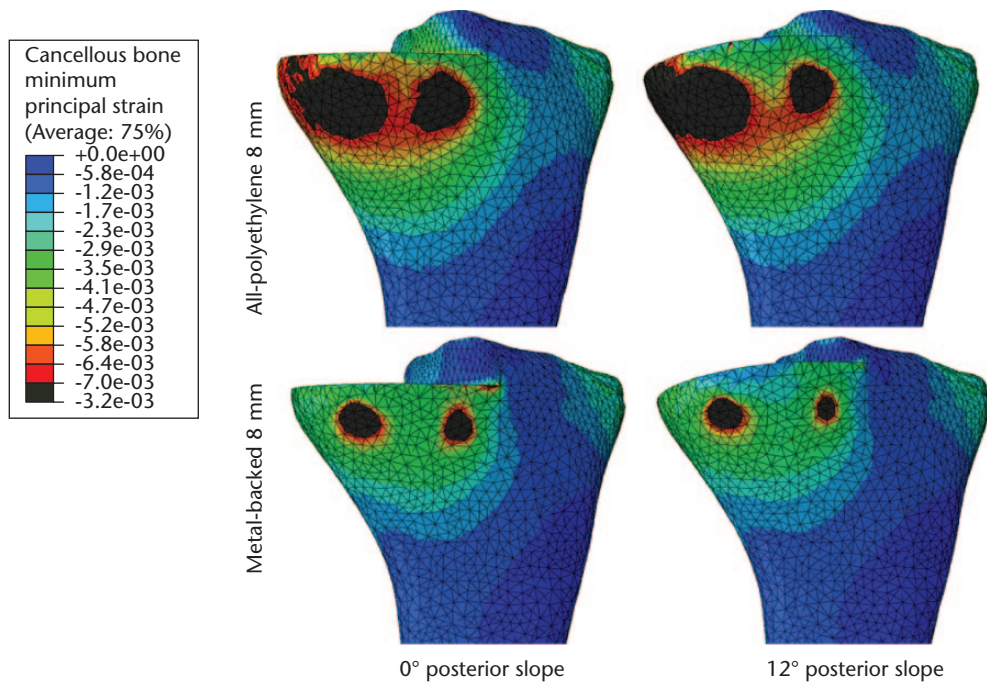


Fig. 7a

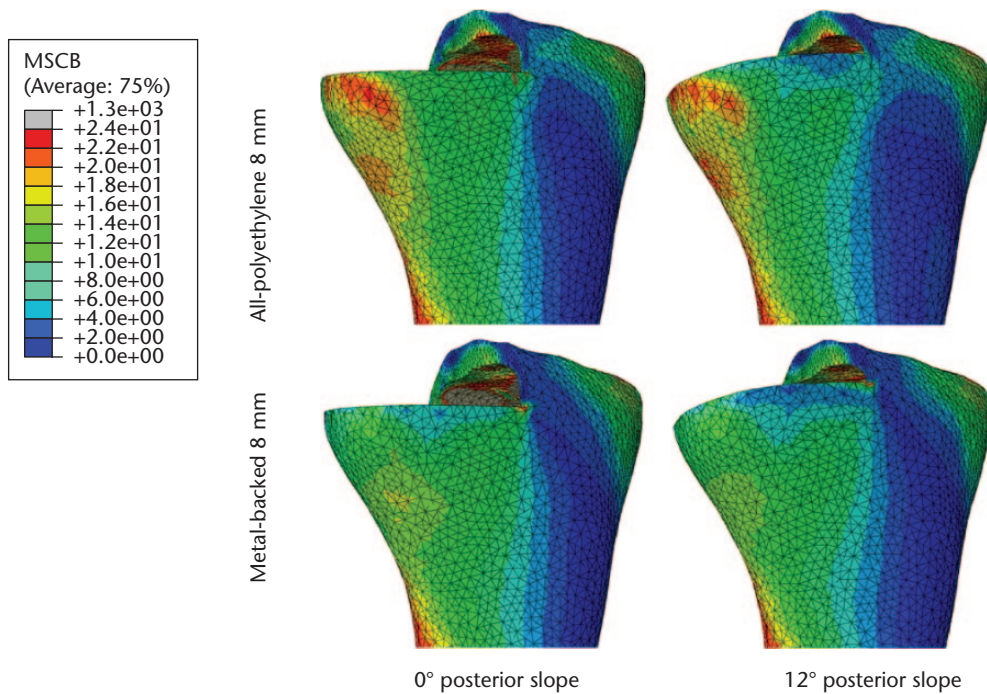


Fig. 7b

a) Cancellous bone minimum principal strain and b) von Mises stress in cortical bone (MSCB) contours for all-polyethylene and metal-backed implants in different sagittal alignments.

market in the United Kingdom)¹ and fixed-bearing UKAs (33% of the market in the United Kingdom).¹ Using MB implants, it remains unclear whether improved alignment of a robotic fixed-bearing UKA translates into superior clinical and patient-reported outcomes compared with a manually inserted mobile-bearing implant, although early

results are promising.²⁷⁻³⁰ Although AP UKAs are more sensitive than MB implants to malalignment, it also appears that associated bone strains for AP implants are higher than those for MB implants, even when perfectly aligned. Robotic-assisted surgery may not therefore provide a resurgence in AP implant use that would exploit the

advantages of these implants in terms of ease of revision;⁷ however, the clinical consequences of elevated strain are uncertain and may be resolved in a number of individuals by bone remodelling.

A linear elastic FEM was used in this study. Although bone is viscoelastic with non-linear behaviour,^{31,32} linear modelling can be used to reduce computing requirements when loading is not cyclical and not to failure.^{19,33} It is argued that yielding and damage in bone is best described using strain rather than stress.³³ Strain-based criteria are numerically more efficient and accurate than stress-based criteria.³³ Previous UKA FEMs report von Mises stress and strains.³⁴⁻³⁶ The threshold limit for cancellous bone strain of 3000 $\mu\epsilon$ was chosen to represent the strain at which cancellous bone is thought to be pathologically overloaded.²¹

The limitations of this study include the use of composite tibias. These do not reflect the graduated trabecular structure of proximal tibial cancellous bone, but are applicable to the 'average' tibia.³⁷ Anisotropic, heterogeneous bone was modelled exhibiting isotropic and homogeneous material properties, and a linearly elastic analysis was performed. This is a common method and does not necessarily discredit the differences found between implants and alignments.¹² The use of strain-based criteria rather than stress-based criteria accommodates for material anisotropy and bone:volume ratio (or porosity). While yield stresses for bone are both anisotropy- and porosity-dependent, yield strains are largely uniform.^{33,38} The threshold used for defining 'overstrain' (-3000 $\mu\epsilon$) is based on evidence^{21,39} and has been used previously,¹² but it is unclear whether this cut-off accurately represents pathological overloading of bone and indeed this threshold may differ by patient. Gait was not modelled. As kinematic studies have shown the point of contact to change little throughout a range of movement in fixed-bearing UKAs, this was considered acceptable.⁴⁰ The soft tissues of the intact lateral compartment were not modelled and this will have affected lateral strain. The medial load was applied directly to the polyethylene, not through a femoral component. Although this is a recognized technique,^{12,14} it may affect the results. In this study, all models were loaded in line with the mechanical axis. In reality, malaligning the implants, especially in extreme cases, may alter the loading axis relative to the native plateau.

In conclusion, this FEM study has shown that UKA tibial component material has a greater effect than malalignment on proximal tibial bone strain. Sagittal plane malalignment has a negligible effect on bone strain for a given load. All-polyethylene implants are more sensitive than MB implants to coronal plane malalignments. Cancellous bone strain and anteromedial cortical bone stress appear to offset one another with varus malalignment, resulting in reduced cancellous bone strain but

increased anteromedial cortical bone stress and *vice versa* in valgus alignment.

References

- No authors listed.** 14th Annual Report. *National Joint Registry*. 2017. <http://www.njrreports.org.uk/Portals/0/PDFdownloads/NJR%2014th%20Annual%20Report%202017.pdf> (date last accessed 31 October 2018).
- No authors listed.** Hip and Knee Arthroplasty Annual Report 2012. *Australian Orthopaedic Association National Joint Replacement Registry*. 2012. <https://aoanjrr.dmac.adelaide.edu.au/documents/10180/60142/Annual%20Report%202012%20version%201.2&t=1355186837517> (date last accessed 31 October 2018).
- Pandit H, Jenkins C, Gill HS, et al.** Minimally invasive Oxford phase 3 unicompartmental knee replacement: results of 1000 cases. *J Bone Joint Surg [Br]* 2011;93-B:198-204.
- Robertsson O, Knutson K, Lewold S, Lidgren L.** The routine of surgical management reduces failure after unicompartmental knee arthroplasty. *J Bone Joint Surg [Br]* 2001;83-B:45-49.
- Liddle AD, Pandit H, Judge A, Murray DW.** Optimal usage of unicompartmental knee arthroplasty: a study of 41,986 cases from the National Joint Registry for England and Wales. *Bone Joint J* 2015;97-B:1506-1511.
- Baker PN, Petheram T, Avery PJ, Gregg PJ, Deehan DJ.** Revision for unexplained pain following unicompartmental and total knee replacement. *J Bone Joint Surg [Am]* 2012;94-A:e126.
- Scott CEH, Powell-Bowns MFR, MacDonald DJ, Simpson PM, Wade FA.** Revision of unicompartmental to total knee arthroplasty: Does the unicompartmental implant (metal-backed vs all-polyethylene) impact the total knee arthroplasty? *J Arthroplasty* 2018;33:2203-2209.
- Simpson DJ, Price AJ, Gulati A, Murray DW, Gill HS.** Elevated proximal tibial strains following unicompartmental knee replacement—a possible cause of pain. *Med Eng Phys* 2009;31:752-757.
- Scott CE, Wade FA, Bhattacharya R, et al.** Changes in bone density in metal-backed and all-polyethylene medial unicompartmental knee arthroplasty. *J Arthroplasty* 2016;31:702-709.
- Small SR, Berend ME, Ritter MA, Buckley CA, Rogge RD.** Metal backing significantly decreases tibial strains in a medial unicompartmental knee arthroplasty model. *J Arthroplasty* 2011;26:777-782.
- Scott CE, Eaton MJ, Nutton RW, et al.** Proximal tibial strain in medial unicompartmental knee replacements: A biomechanical study of implant design. *Bone Joint J* 2013;95-B:1339-1347.
- Scott CE, Eaton MJ, Nutton RW, et al.** Metal-backed versus all-polyethylene unicompartmental knee arthroplasty: proximal tibial strain in an experimentally validated finite element model. *Bone Joint Res* 2017;6:22-30.
- Sawatari T, Tsumura H, Iesaka K, Furushiro Y, Torisu T.** Three-dimensional finite element analysis of unicompartmental knee arthroplasty—the influence of tibial component inclination. *J Orthop Res* 2005;23:549-554.
- Simpson DJ, Gray H, D'Lima D, Murray DW, Gill HS.** The effect of bearing congruency, thickness and alignment on the stresses in unicompartmental knee replacements. *Clin Biomech (Bristol, Avon)* 2008;23:1148-1157.
- Zhu GD, Guo WS, Zhang QD, Liu ZH, Cheng LM.** Finite element analysis of mobile-bearing unicompartmental knee arthroplasty: The influence of tibial component coronal alignment. *Chin Med J (Engl)* 2015;128:2873-2878.
- Scott CEH, Wade FA, Bhattacharya R, et al.** Changes in bone density in metal backed and all-polyethylene medial unicompartmental knee arthroplasty. *J Arthroplasty* 2016;31:702-709.
- Paley D.** Normal limb alignment and joint orientation. In: Herzenberg JE ed. *Principles of Deformity Correction*. New York: Springer, 2002:1-18.
- Completo A, Rego A, Fonseca F, et al.** Biomechanical evaluation of proximal tibia behaviour with the use of femoral stems in revision TKA: an in vitro and finite element analysis. *Clin Biomech (Bristol, Avon)* 2010;25:159-165.
- Conlisk N, Howie CR, Pankaj P.** The role of complex clinical scenarios in the failure of modular components following revision total knee arthroplasty: A finite element study. *J Orthop Res* 2015;33:1134-1141.
- Kutzner I, Heinlein B, Graichen F, et al.** Loading of the knee joint during activities of daily living measured in vivo in five subjects. *J Biomech* 2010;43:2164-2173.
- Frost HM.** Strain and other mechanical influences on bone strength and maintenance. *Curr Opin Orthop* 1997;8:60-70.
- Furnes O, Espehaug B, Lie SA, et al.** Failure mechanisms after unicompartmental and tricompartmental primary knee replacement with cement. *J Bone Joint Surg [Am]* 2007;89-A:519-525.

23. **Mariani EM, Bourne MH, Jackson RT, Jackson ST, Jones P.** Early failure of unicompartmental knee arthroplasty. *J Arthroplasty* 2007;22(6 Suppl 2):81-84.
24. **Hamilton WG, Collier MB, Tarabee E, et al.** Incidence and reasons for reoperation after minimally invasive unicompartmental knee arthroplasty. *J Arthroplasty* 2006;21(6 Suppl 2):98-107.
25. **Scott CEH, Wade FA, MacDonald D, Nutton RW.** Ten-year survival and patient-reported outcomes of a medial unicompartmental knee arthroplasty incorporating an all-polyethylene tibial component. *Arch Orthop Trauma Surg* 2018;138:719-729.
26. **Bell SW, Anthony I, Jones B, et al.** Improved accuracy of component positioning with robotic-assisted unicompartmental knee arthroplasty: Data from a prospective, randomized controlled study. *J Bone Joint Surg [Am]* 2016;98-A:627-635.
27. **Blyth MJG, Anthony I, Rowe P, et al.** Robotic arm-assisted versus conventional unicompartmental knee arthroplasty: Exploratory secondary analysis of a randomised controlled trial. *Bone Joint Res* 2017;6:631-639.
28. **Gilmour A, MacLean AD, Rowe PJ, et al.** Robotic-arm-assisted vs conventional unicompartmental knee arthroplasty. The 2-year clinical outcomes of a randomized controlled trial. *J Arthroplasty* 2018;33:S109-S115.
29. **Kayani B, Konan S, Tahmassebi J, Pietrzak JRT, Haddad FS.** Robotic-arm assisted total knee arthroplasty is associated with improved early functional recovery and reduced time to hospital discharge compared with conventional jig-based total knee arthroplasty. *Bone Joint J* 2018;100-B:930-937.
30. **Kayani B, Konan S, Pietrzak JRT, et al.** The learning curve associated with robotic-arm assisted unicompartmental knee arthroplasty. *Bone Joint J* 2018;100-B:1033-1042.
31. **Manda K, Xie S, Wallace RJ, Levrero-Florencio F, Pankaj P.** Linear viscoelasticity - bone volume fraction relationships of bovine trabecular bone. *Biomech Model Mechanobiol* 2016;15:1631-1640.
32. **Manda K, Wallace RJ, Xie S, Levrero-Florencio F, Pankaj P.** Nonlinear viscoelastic characterization of bovine trabecular bone. *Biomech Model Mechanobiol* 2017;16:173-189.
33. **Pankaj P, Donaldson FE.** Algorithms for a strain-based plasticity criterion for bone. *Int J Numer Methods Biomed Eng* 2013;29:40-61.
34. **Kwon OR, Kang KT, Son J, et al.** Biomechanical comparison of fixed- and mobile-bearing for unicompartmental knee arthroplasty using finite element analysis. *J Orthop Res* 2014;32:338-345.
35. **Gray HA, Zavatsky AB, Taddei F, Cristofolini L, Gill HS.** Experimental validation of a finite element model of a composite tibia. *Proc Inst Mech Eng H* 2007;221:315-324.
36. **Gray HA, Taddei F, Zavatsky AB, Cristofolini L, Gill HS.** Experimental validation of a finite element model of a human cadaveric tibia. *J Biomech Eng* 2008;130:031016.
37. **Cristofolini L, Viceconti M.** Mechanical validation of whole bone composite tibia models. *J Biomech* 2000;33:279-288.
38. **Levrero-Florencio F, Margetts L, Sales E, et al.** Evaluating the macroscopic yield behaviour of trabecular bone using a nonlinear homogenisation approach. *J Mech Behav Biomed Mater* 2016;61:384-396.
39. **Frost HM.** Some ABC's of skeletal pathophysiology. 5. Microdamage physiology. *Calcif Tissue Int* 1991;49:229-231.
40. **Argenson JN, Komistek RD, Aubaniac JM, et al.** In vivo determination of knee kinematics for subjects implanted with a unicompartmental arthroplasty. *J Arthroplasty* 2002;17:1049-1054.

Author contributions

- I. Danese: Performed the finite element modelling and analysis, Interpreted the data, Wrote the manuscript.
- P. Pankaj: Designed the study, Interpreted the data, Wrote the manuscript.
- C. E. H. Scott: Designed the study, Developed the finite element model, Interpreted the data, Wrote the manuscript.

Funding statement

- The authors acknowledge the financial support of NHS Research Scotland (NRS), through C. E. H. Scott of NHS Lothian. In addition, P. Pankaj reports funding from the Engineering and Physical Sciences Research Council (EPSRC).
- No benefits in any form have been received or will be received from a commercial party related directly or indirectly to the subject of this article.

© 2019 Author(s) et al. This is an open-access article distributed under the terms of the Creative Commons Attributions licence (CC-BY-NC), which permits unrestricted use, distribution, and reproduction in any medium, but not for commercial gain, provided the original author and source are credited.